

Optic Disc and Cup Boundary Segmentation for Glaucoma Screening in Fundus Image

R. Shanthi and S. Prabakaran

Department of Computer Science and Engineering, SRM Institute of Science and Technology,
Chennai, Tamil Nadu, India

Abstract: Automatic and accurate localization of Optic Disk and Cup (ODC) in retinal fundus image is a necessary process for diagnosis of glaucoma. Glaucoma is the second leading chronic eye disorder which harms the optic nerve head and causes vision loss which leads to permanent blindness. The glaucoma can be detected by segmenting ODC boundary and calculating the Ratio of optic Disc and Cup (CDR). This study presents an effective framework for automatic segmentation of ODC boundary. The framework begins with median filtering to smoothen the original fundus image, followed by region of interest is marked, next superpixel is generated using SLIC method, finally, Hough transform circle and Otsu's threshold method is used to detect the optic disc and cup boundary. Drive online public dataset is used to assess the performance of the proposed system. The average precision, recall and F-score values obtained for detecting optic disc are 0.98, 0.97 and 0.95, respectively and for optic cup a precision, recall and F-score values are 0.92, 0.95 and 0.93, respectively. The experiment results achieved is showed that the proposed technique gives better result in segmenting the boundary of optic disc and cup in retinal fundus image.

Key words: Glaucoma, Optic Disc and Cup (ODC), segmentation, superpixel, Simple Linear Iterative Cluster (SLIC), Circular Hough Transform (CHT)

INTRODUCTION

Eye is the beautiful and sensory organ that facilitate us to direct our way through the globe. Glaucoma is the complex eye disorder which is most commonly examined among diabetic patients. Diabetes leads to growth of blood vessel in the drainage route of the eye which raises eye pressure called Intraocular Pressure (IOP) and causes glaucoma. It is a leading chronic disorder often named as silent thief of sight. It does not produces any symptoms and it gets worse overtime which causes long-lasting blindness, if it is not detected and treated at an premature stage. Clinical treatment is essential and normally aimed at preventing further loss. The World Health Organization (WHO) has declared glaucoma as the second major cause of loss of sight all over the world and it includes 15% of the vision loss cases in the world which creates 5.2 million of the world's popuslation (Thylefors and Negrel, 1994) and it is expected to raise up to 80 million by 2020(Quigley and Broman, 2006). According to the statistics, the occurrence rate of the people affected by the disease glaucoma and their respective age is given in Fig. 1. From 2010-2050, the people in US

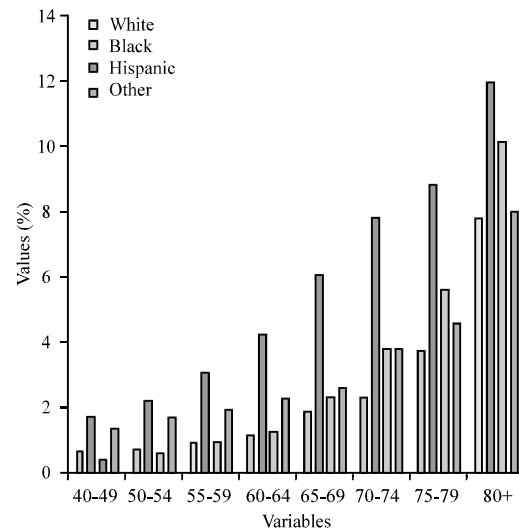


Fig. 1: Glaucoma affected people and age (Almekinder, 2018) (prevalence rates for glaucoma by age and race)

with glaucoma is expected to rise by more than double from 2.7-6.3 million is shown in Fig. 2 (Almekinder, 2018).

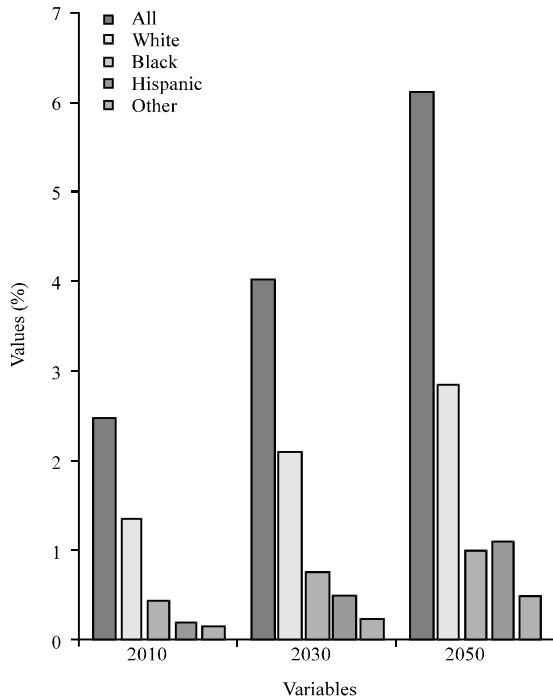


Fig. 2: Projections for glaucoma (Almekinder, 2018) (in 2030 and 2050 in millions)

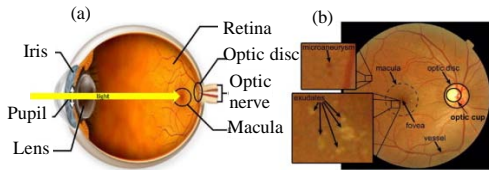


Fig. 3: a) Anatomy of human eye and b) Anatomy of fundus image

The fundus is the cross-sectional interior surface view of the eye, straight opposite to the lens and it comprises the optic disc, optic cup, blood vessel, macula and fovea. The anatomy of human eye and fundus image is shown in Fig. 3 and it is examined through fundus photography or by ophthalmoscopy. The optic disc or optic nerve is in elliptic circle in shape and it is the brightest region in the fundus image. Optic disc is the blind spot area where the optic nerve and blood vessel enters into the retina. The optic disc can have a certain amount of normal cupping. When the glaucoma arises the cup enlarges and occupies most of the area of disc (Anonymous, 2012a, b). The normal eye optic disc diameter vertically and horizontally is estimated as 1.88 and 1.77 mm. The optic cup is the cup like area in the mid of optic disc. The Cup to Disc Ratio (CDR) is a measurement used to assess the progression of glaucoma

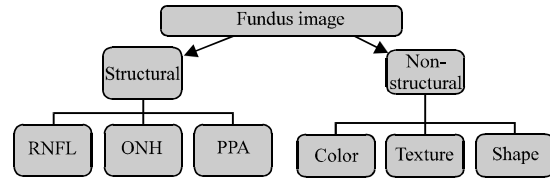


Fig. 4: Feature extraction method

which is the ratio of the vertical height of the optic cup and optic disc. The normal human eye cup to disc ratio is 0.3 and it is widely acceptable up to 0.5. When it exceeds, a large cup to disc ratio implies other pathology or glaucoma (Anonymous, 2012a, b). The macula is the small flat spot light sensitive layer of tissue lining the inside of the rear end of the eye. A small pit located in the macula that provides clearest vision is fovea. The blood vessel is one of the important feature in the fundus image, the convergence of the blood vessel is optic nerve head. The diameter of the vessel around the optic disc is about 150 μm. Researchers and clinicians use this feature for disease diagnosis.

The segmentation or feature extraction method can be classified into structural and non-structural. Structural features have been carried out by using some feature extraction method such as Retinal Nerve Fiber Layer (RNFL) thickness, Optic Nerve Head (ONH) Peripapillary Atrophy (PPA) method and non-structural feature extraction methods such as pixel intensity, texture and shape features are carried out for examination. Our proposed technique uses non-structural method to improve the accuracy of segmenting optic disc and cup in fundus image (Fig. 4).

Literature review: Joshi *et al.* (2011) segmented the optic disk and cup from monocular color fundus Images using contour model based on anatomical evidence such as blood vessels turns at the cup boundary for glaucoma assessment. This method is not preferable with abnormal fundus image which does not have proper blood vessel turns in the retina. Mahfouz and Fahmy (2009) proposed ultrafast localization of the optic disc using reduction in dimensionality of the search space. Initially macula is detected then optic disc position is found out by calculating the distance between macula and OD. But the distance between macula and OD may vary in some instance. The major issue in this method is misdetection of OD due to swollen optic nerve and another issue is it is unnecessary to detect macula’s position to detect optic disc position. Niemeijer *et al.* (2006) presented an automatic system is to find the location of optic disc,

blood vascular and macula in the major anatomical structures in color fundus image. The segmentation of OD is done by examining the vasculature network inside the retina but it is so tedious and time-consuming process to validate the whole, vascular network. Fraga *et al.* (2011) presented contrast normalization and luminosity by multiscale retinex algorithm. In order to find the location of OD fuzzy convergence and fuzzy Hough transform is applied and for segmenting OD canny filter and ROI is used.

Welfer *et al.* (2010) proposed a new adaptive technique based on the model of vascular structure, mathematical morphology and watershed algorithm for automatic segmentation of OD. Aquino *et al.* (2010) proposed morphological processing method for eliminating blood vessels, binary mask to obtain OD boundary candidates and circular Hough transform for OD boundary segmentation. Tjandrasa *et al.* (2012) proposed homomorphic filtering, Hough transform and initial active contours for blood vessel removal and segmenting optic disc. Yin *et al.* (2011) have proposed a novel method that consists of detecting the edges, circular Hough transform and statistical deformable model to segment the boundary of OD. Cheng *et al.* (2011) proposed ROI and edge filtering for preprocessing, •-PPA detection and constrained elliptical Hough transform for postprocessing process for OD boundary detection and segmentation. Zhang *et al.* (2012) used Gabor filtering and multithreshold processing for vessel detection, horizontal location of OD and vertical location of OD is detected using vascular scatter degree and edge gradient degree. Youssif *et al.* (2007) proposed Adaptive Histogram Equalization (AHE) to normalize and enhance

the contrast, vessel's direction matched filter is applied to track the blood vessel direction convergence to detect the OD location.

MATERIALS AND METHODS

The main objective of this study is to segment the optic disc and cup region with latest efficient methods which will help to detect glaucoma. The workflow is as follows.

Image acquisition: Initially an input RGB fundus image is retrieving from drive public online data source. Some of the other online datasets are Origa Stare, Diaret DB0, Diaret DB1, Messidor, etc.

Pre-processing: The input RGB fundus image is converted into gray level image, so that, many operations can be done easily in gray level image than RGB images.

Segmentation: Segmentation of optic disc and optic cup are to done using various operations to detect their boundaries (Fig. 5).

Preprocessing: Preprocessing is the important initial technique applied to the raw input RGB fundus image to remove the noise, unwanted features established during image acquisition, uneven contrast or illumination etc. The input RGB fundus image is converted into grey level image by taking the luminosity method, it averages the RGB values and it figures a weighted average, since, researchers are more sensitivity in green color than other

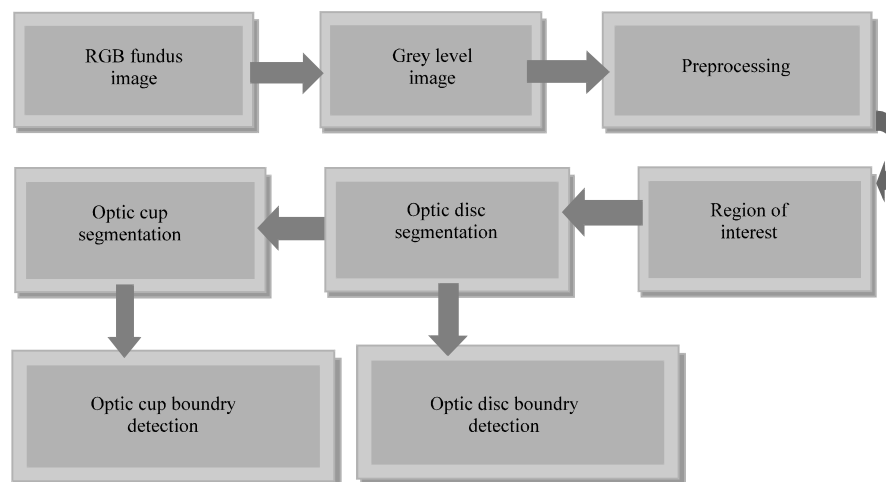


Fig. 5: Workflow of proposed system

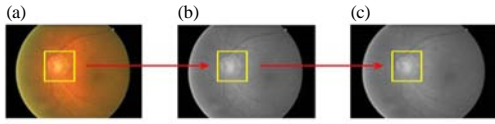


Fig. 6: a) Color fundus image; b) Grey level fundus image and c) Preprocessed median filtering image

colors, so, green is weighted most heavily. The formula for calculating luminosity method is $0.21 R + 0.72 G + 0.07 B$. By this researchers can get the grey image converted form to make further process easily. In Fig. 6b shows how the color fundus image is converted into grey level image and this is taken as an input for next level process.

Median filtering: Median filter is a smoothing non linear local filtering technique widely used in digital image processing and gives better result in preprocessing by removing the speckle noise and salt and pepper noise completely. Instead of taking average or mean, median is taken by sorting the pixel values from small to big and taking the middle (median) value. The average value will be taken as a median in case of two values in center position. When suppressing noise in smooth regions, other filtering algorithms are worse in preserving edges but median filter research better in reducing noise and at the same time it does not affect the edges from the filter window. Its performance is much better when the noise level is between low to moderate. Features that is lesser than half the range of median filter is entirely removed by the filter. Large discontinuities like edges and large varies in image intensity does not affect in terms of gray-level intensity by the median filtering method, though their places may be shifted by few pixels. This nonlinear technique of the median filter allows significant suppression of particular types of noise. For example, “pepper -and- salt noise” may be removed entirely from an image with no attenuation of important image edges or characteristics. The median filtering technique can applied and calculated using the given Eq. 1. Fig. 6c shows the output of applying the median filter image from the grey level image:

$$f(x, y) = \text{median} \{g(s, t)\} \quad (1)$$

where (s, t) belongs to S_{xy} , S_{xy} is a set of coordinates in a image window which has a midpoint at (x, y) , here, the median filter calculates the median of the corrupted fundus image $g(x, y)$ under the area S_{xy} , here, $f(x, y)$ represents the restored fundus image (Algorithm 1). The procedure to apply median filtering is as follows:

Algorithm 1; The procedure to apply median filtering:

```

allocate outputPixValue[image width][image height]
allocate window>window width * window height]
xedge: = (window width/2) rounded down
yedge: = (window height/2) rounded down
for x from xedge to image width - xedge
for y from yedge to image height - yedge
i = 0
for fx from 0 to window width
for fy from 0 to window height
window[i]: = inputPixValue[x + fx - xedge][y+fy-yedge]
I: = i+1
sort entries in window[]
outputPixValue[x][y]: = window>window width * window height /2]
    
```

Optic disc segmentation: Optic disc boundary segmentation is a extremely challenging job because of blood vessel blockages, inconsistent imaging conditions, blood vessel occlusions, pathological conditions in the region of disc, etc. This study describes the three major mechanism of the model: the region selection of the ROI in the training images and the SLIC clustering technique is applied on ROI descriptors to detect the edges. It is not sufficient to optimize the detection of optic disc and cup location over the combination of ROI and the pixel intensity based clustering technique. When using pixel intensity based detection technique there may be a chance of detection false region due to microaneurysms or hemorrhages. The microaneurysms is a sign of diabetic retinopathy which have a part of damaged eye tissue, this causes swelling in the blood vessel and fluffy patches occur in retina in case of bright lesions called hemorrhages (Shanthi and Prabakaran, 2018). To avoid that Hough transform circle and Otsu’s thresholding method are applied to find the exact location of optic disc and cup detection.

Region of interest: Localization of disc and cup is a very significant step to detect the glaucoma disease. In order to segment the optic disc and cup, the region of interest is to be detected, instead of finding out the disc intensity pixels in the entire fundus image an alternative method is to focus only on the region to concentrate. The area or region containing disc pixel is the required region of interest. If the region is detected correctly, the complete size of the image is reduced into smaller image which helps to quicken the process of segmenting disc and cup boundary. ROI algorithms apply any of the approaches like feature based or object based method. Feature based approach discover pixels that share important optical features with the threshold and combined them to form ROIs (Privitera and Stark, 2000). Whereas object-based approach detect ROIs at a advanced level than the pixel by pixel method of feature based systems using information such as target structure and shape (Stough and Brodley, 2001). It is known that the optic disc

region has higher intensity when comparing to other area of the fundus image. A rough high intensity region is calculated by means of correlation coefficient between original and mask image. A rectangle portion doubles the diameter of the optic disc is marked around the ROI is called ROI boundary which is used for segmenting optic disc and cup. The algorithm to find the location of disc is as follows:

- The original image *s* resized into 256×256
- Median filtering smoothing non linear local filter is applied in preprocessing to remove noise
- Binary image was produced by taking threshold value
- Morphological operation to binary image is applied
- The basic properties of the region are calculated
- Correlation coefficient between the input and mask image is calculated
- The required region of interest pixels is found and marked for further process

Simple linear iterative clustering approach: Simple Linear Iterative Clustering (SLIC) is fast to compute, reduces the computational complexity, simple to understand, efficient and excellent when compared to other super pixel methods. Achanta *et al.* (2012) many features such as color, location, appearance and texture can be extracting from super pixels for classification. Color histogram from super pixels is an intuitive option for feature extraction. Cheng *et al.* (2012) SLIC algorithm is used to aggregate the nearby pixels into super pixels in fundus image and it research well in segmentation process to increase the excellence in the aspect of producing results. It makes a neighboring clustering of pixels in 5D space defined by *L*, *a*, *b* values of the CIELAB color space and *x*, *y* coordinates of the pixels. SLIC produces superpixels by clustering pixels based on their similarity of color and proximity in image plane. A 5 dimensional [labxy] space is used for clustering. SLIC gets a preferred number of approximately equally-sized superpixels *K* as an input. Subsequently, each superpixels will have roughly *N/K* pixels. Therefore, for all equally sized superpixels, there would be a superpixel center at each grid interval *S* • (*N/K*). The centers are stimulated to seed the locations corresponding to the lowest gradient position in a 3×3 neighborhood. *K* superpixel cluster centers $C_k = [l_k, a_k, b_k, x_k, y_k]^T$ with *k* = [1, *K*] at regular grid intervals *S* are selected. It can be understood that the pixels associated with the cluster lie in 2*S*×2*S* area around the superpixel center in the *xy* plane because the spatial extent of any cluster is approximately *S*². To compute a residual error *E*, L2 norm is used between the new cluster center and

previous cluster center locations. This can be repeated iteratively until the error converges. Euclidean distances in CIELAB color space are meaningful for short distances. If spatial pixel distances go beyond the perceptual color distance limit, then they start to outweigh pixel color similarities. The Distance measure *D_s* is described in the Eq. 2-4 as follows:

$$d_{lab} = \sqrt{((l_k - l_i)^2 + (a_k - a_i)^2 + (b_k - b_i)^2)} \quad (2)$$

$$d_{xy} = \sqrt{((x_k - x_i)^2 + (y_k - y_i)^2)} \quad (3)$$

$$D_s = d_{lab} + (m/S) * d_{xy} \quad (4)$$

Where:

D_s = The sum of the lab distance

xy = Plane distance normalized by the grid interval *S*

m = Established in *D_s* allowing us to control the superpixel compactness

The greater the value of *m*, the more spatial proximity is emphasized and the more compact the cluster. This value can be in the range (Achanta *et al.*, 2012). The SLIC segmentation Algorithm 2 is as follows:

Algorithm 2; SLIC segmentation:

```

/* Initialization */
Initialize the cluster centers  $C_k = [l_k, a_k, b_k, x_k, y_k]^T$  by sampling pixels on regular grid steps S
Move centers to the lowest gradient position in a 3x3 neighborhood
Set label l(i) = -1 for each pixel i
Set distance d(i) = ∞ for each pixel i
repeat
/* Assignment */
for each cluster center Ck do
for each pixel i in a 2S×2S region around Ck do
Compute the distance D between Ck and i
If D < d(i) then
set d(i) = D
set l(i) = k
end if
end for
end for
/* Update */
Compute new cluster centers
Compute residual error E
until E • threshold
    
```

Hough transform circle: Since, the optic disk is in circular shape, Circle Hough Transform (CHT) is used for detecting the optic disc area. CHT is an efficient method to detect the circles in image. The circular object among the connected components is referred as (CO) the centroid of CO which is close to the circle centre detected by the CHT is chosen as the centre point of the optic disc. A circle can be distorted into a set of 3 parameters, representing its radius and centre. A circular shape is described by the parametric equation in Eq. 5.

$$(x - p)^2 + (y - q)^2 = r^2 \tag{5}$$

Where:

- (p, q) = The center of circle
- r = The radius of circle
- (x, y) = The pixels coordinates

An accumulator space is created first which is made up of a cell for each pixel, initially, all these values are set to zero. For all edge point in image (x, y) all cells are incremented, according to Eq. 5 which could be the circle centroid. These cells are characterized by 'p'. All possible values of 'q' are found for all possible values of 'p' found in previous step. The cells having the highest maximum probability of being the location of the required circle are searched. These are the cells whose value is higher than its neighborhood cells. An accumulator space has peaks where circles obtained from each edge point overlap at centers of any circles detected. The maximum accumulator value is then found out which corresponds to radius that matches the OD and corresponding center is detected as OD center. The parametric representation of the circle is given by:

$$x = p + r \cos(\theta), y = q + r \sin(\theta) \tag{6}$$

The corresponding connected component chosen with the centroid forms the original optic disc. The optic disc area and boundary positions are obtained. A Bounding Box (BB) is estimated for the optic disc segmented. The ROI which is the optic disc is cropped from the original image for further optic cup segmentation. Optic disc segmentation Algorithm 3 is as follows:

Algorithm 3; Optic disc segmentation:

```

Obtain all the Connected Components (CC) from a mask image M
Detect all the circle objects among the connected components (CO) by circle
detection Hough transform
For all the CCI in M
For all the COi in M
if (centroid(CCI) is equal to centroid (COi)
  optic disc_center is equal to centroid (CCI)
  optic disc_area = area (COi)
  estimate the Bounding Box (BB) for CCI to be used for cup segmentation
else
  eliminate the CCI from M
    
```

The optic cup which is present within the optic disc region which is not always in circular shape and its shape also, varies with the affected eye. To segment the optic disc morphological closing operation is performed on the image which smoothens the boundary, eliminates small holes and fills the gaps in the boundary. The closing operation (\bullet) is defined as follows:

$$I \bullet S = (I \oplus S) \vee S \tag{7}$$

Where:

- I = The input image
- S = The circular structuring element

The structuring element is defined based on the shape of object to detect and probes an image using hit or fit operations. In Eq. 7, \bullet denotes dilation which is used for thickening the boundary of the object interest and \vee denotes erosion which is used to shrinking/thinning the boundary. The extent of thickening and thinning is a function of shape of the structuring element used. The morphological dilation and erosion are defined in Eq. 8 and 9, respectively (Algorithm 4):

$$I \oplus S = \{z | (S^{\wedge})Z \cap I \neq \Phi\} \tag{8}$$

$$I \vee S = \{z | (S)Z \subseteq I\} \tag{9}$$

Where:

- S = The set of pixels
- (S)z = Translation of a set S by point z with (z1, z2) whose (x, y) coordinates have been replaced by (x+z1, +y+z2)
- (S $^{\wedge}$) = Denotes reflection on S set whose (x, y) coordinates are replaced by (-x, -y)

Algorithm 4; The steps involved in optic cup segmentation:

```

Create a disk-shaped Structuring Element (SE) with radius 10
Obtain a resultant image by executing morphological closing operation
using SE on BB
Extract green channel from the resultant image
Perform Otsu's thresholding on the green channel to segment the optic cup
    
```

The optic disc segmentation is processed by dilation process followed by erosion operation using a circular structuring element. Now from the morphologically altered image, the green channel is separated and then the Otsu's thresholding method is applied which gives the boundary position and the area of the optic cup.

RESULTS AND DISCUSSION

The experiment of the proposed method is carried out using DRIVE (Digital Retinal Images for Vessel Extraction) dataset. The sample results of various stages such as preprocessing, superpixel generation, optic disc boundary segmentation, optic cup segmentation and optic optic disc and cup boundary segmentation is shown in Fig. 7.

The boundary detection similarity is done by the evaluation process. The area overlap between computed and ground truth area was computed by precision and recall values using Eq. 10 and 11. The other method of measuring the performance is done through the value of F-score and this value should lie between 0-1. The formula

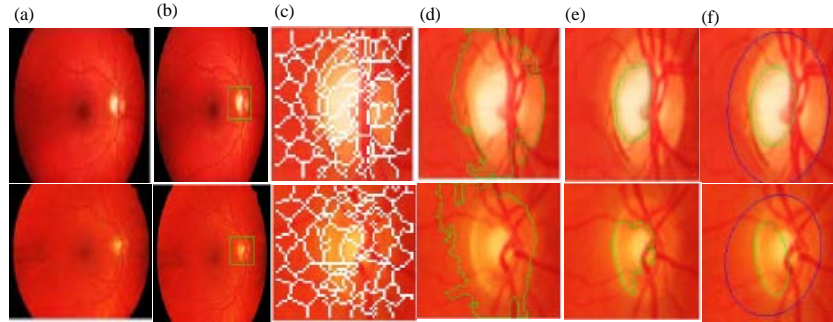


Fig. 7: a) Original fundus image; b) Region of interest; c) Super pixel generation; d) Optic disc boundary; e) Optic cup boundary and f) ODC boundary segmentation

Table 1: Test image values of optic disc and cup boundary

Test images	Optic disc values			Optic cup values		
	Precision	Recall	F-score	Precision	Recall	F-score
1	0.97	0.95	0.93	0.9	0.94	0.92
2	0.98	0.98	0.94	0.92	0.96	0.93
3	0.99	0.98	0.94	0.93	0.97	0.94
4	0.97	0.97	0.97	0.92	0.96	0.92
5	0.97	0.95	0.94	0.92	0.95	0.96
6	0.98	0.99	0.93	0.92	0.98	0.92
7	0.96	0.96	0.94	0.91	0.96	0.96
8	0.97	0.97	0.95	0.91	0.97	0.93
9	0.99	0.98	0.95	0.91	0.94	0.91
10	0.98	0.97	0.96	0.91	0.91	0.91

Table 2: Comparison of experimental results

Techniques	Precision	Recall	F-score
Hausdorff-based template	0.94	0.71	0.81
Morphological method	0.77	0.83	0.80
Supervised method	0.98	0.70	0.82
SVM	0.85	0.84	0.84
Fuzzy convergence	0.99	0.85	0.91
Active contour method	0.72	0.82	0.81
Medial axis detection method	0.90	0.96	0.93
Proposed method	0.98	0.97	0.95

for calculating F-score is given in Eq. 12. The 10 samples of drive dataset results of precision, recall and F-score values is shown in Table 1 for both optic disc and cup boundary. The proposed system result of optic disc boundary is compared with other existing techniques and it shows better performance than the existing technique is shown in Table 2:

$$\text{Precision} = \text{TP} / (\text{TP} + \text{FP}) \quad (10)$$

$$\text{Recall} = \text{TP} / (\text{TP} + \text{FN}) \quad (11)$$

$$F = 2 * ((\text{Precision} * \text{Recall}) / (\text{Precision} + \text{Recall})) \quad (12)$$

Where:

TP = The number of True Positive pixels

FP = The number of False Positive pixels

FN = The number of False Negative pixels

CONCLUSION

The main objective of segmenting optic disc and optic cup in the fundus image is to find out the early detection of glaucoma. The symptoms of this disease occur only when the disease is in quite advance, this leads to permanent loss of vision, so, early detection of glaucoma is very essential. The proposed system implemented superpixel based method to find the disc region, circular Hough transform and thresholding method for segmenting optic disc and cup boundary. The Cup-to-Disc Ratio (CDR) is acknowledged as a record for the evaluation of glaucoma (Shanthi and Prabakaran, 2019). It has been proved that the proposed method is an efficient method and beneficial method which gives finest result with increased performance and reduced computations. The proposed method is tested in drive dataset. The results of various existing techniques are compared and it is found that the proposed technique is greater in terms of accuracy and computational time. The precision, recall and F-score of the identified optic disc boundary values are 0.98, 0.97 and 0.95 and the cup boundary is 0.92, 0.95 and 0.93. This technique is restricted to only drive dataset, in future this can be extended to larger dataset to segment the optic disc and cup boundary at the utmost level cup using deep learning method.

REFERENCES

- Achanta, R., A. Shaji, K. Smith, A. Lucchi and P. Fua *et al.*, 2012. SLIC super pixels compared to state-of-the-art super pixel methods. *IEEE. Trans. Pattern Anal. Mach. Intell.*, 34: 2274-2282.
- Almekinder, R.N.E., 2018. Gallup report shows diabetes increasing at disturbing rates in the US. *The Diabetes Council.com., USA.* <https://www.thediabetescouncil.com/>

- Anonymous, 2012a. Eye exam and tests for glaucoma diagnosis. The Eye Digest, University of Illinois Eye and Ear Infirmary, Chicago, Illinois, USA.
- Anonymous, 2012b. Glaucoma causes optic nerve cupping (atrophy) and vision loss. The Eye Digest, University of Illinois Eye and Ear Infirmary, Chicago, Illinois, USA. <https://web.archive.org/web/20120708075410/http://www.agingeye.net/glaucoma/glaucomainformation.php>
- Aquino, A., M.E. Gegundez-Arias and D. Marin, 2010. Detecting the optic disc boundary in digital fundus images using morphological, edge detection and feature extraction techniques. *IEEE Trans. Med. Imag.*, 29: 1860-1869.
- Cheng, J., J. Liu, D.W.K. Wong, F. Yin and C. Cheung *et al.*, 2011. Automatic optic disc segmentation with peripapillary atrophy elimination. Proceedings of the 2011 Annual International Conference on IEEE Engineering in Medicine and Biology Society (EMBC'11), August 30-September 3, 2011, IEEE, Boston, Massachusetts, USA., ISBN:978-1-4244-4121-1, pp: 6224-6227.
- Cheng, J., J. Liu, Y. Xu, F. Yin and D.W.K. Wong *et al.*, 2012. Superpixel classification for initialization in model based optic disc segmentation. Proceedings of the 2012 Annual International Conference on IEEE Engineering in Medicine and Biology Society, August 28-September 1, 2012, IEEE, San Diego, California, USA., ISBN:978-1-4244-4119-8, pp: 1450-1453.
- Fraga, A., N. Barreira, M. Ortega, M.G. Penedo and M.J. Carreira, 2011. Precise segmentation of the optic disc in retinal fundus images. Proceedings of the International Conference on Computer Aided Systems Theory (EUROCAST 2011), February 6-11, 2011, Springer, Berlin, Germany, ISBN: 978-3-642-27548-7, pp: 584-591.
- Joshi, G.D., J. Sivaswamy and S.R. Krishnadas, 2011. Optic disk and cup segmentation from monocular color retinal images for glaucoma assessment. *IEEE. Trans. Med. Imag.*, 30: 1192-1205.
- Mahfouz, A.E. and A.S. Fahmy, 2009. Ultrafast localization of the optic disc using dimensionality reduction of the search space. Proceedings of the 12th International Conference on Medical Image Computing and Computer-Assisted Intervention: Part II (MICCAI 2009) Vol. 5762, September 20-24, 2009, ACM, London, UK., ISBN:978-3-642-04270-6, pp: 985-992.
- Niemeijer, M., M.D. Abramoff and B.V. Ginneken, 2006. Segmentation of the optic disc, macula and vascular arch in fundus photographs. *IEEE. Trans. Med. Imaging*, 26: 116-127.
- Privitera, C.M. and L.W. Stark, 2000. Algorithms for defining visual regions-of-interest: Comparison with eye fixations. *IEEE. Trans. Pattern Anal. Mach. Intell.*, 22: 970-982.
- Quigley, H.A. and A.T. Broman, 2006. The number of people with glaucoma worldwide in 2010 and 2020. *Br. J. Ophthalmol.*, 90: 262-267.
- Shanthi, R. and S. Prabakaran, 2018. Detection of microaneurysms and hemorrhages in fundus image for glaucoma diagnosis. *Int. J. Eng. Technol.*, 7: 391-396.
- Shanthi, R. and S. Prabakaran, 2019. Effective utilization of artificial intelligence for predicting glaucoma in fundus image. *Caribbean J. Sci.*, 53: 902-912.
- Stough, T.M. and C.E. Brodley, 2001. Focusing attention on objects of interest using multiple matched filters. *IEEE. Trans. Image Process.*, 10: 419-426.
- Thylefors, B. and A.D. Negrel, 1994. The global impact of glaucoma. *Bull. World Health Organ.*, 72: 323-326.
- Tjandrasa, H., A. Wijayanti and N. Suciati, 2012. Optic nerve head segmentation using Hough transform and active contours. *Telkomnika*, 10: 531-536.
- Welfer, D., J. Scharcanski, C.M. Kitamura, M.M.D. Pizzol and L.W.B. Ludwig *et al.*, 2010. Segmentation of the optic disk in color eye fundus images using an adaptive morphological approach. *Comput. Biol. Med.*, 40: 124-137.
- Yin, F., J. Liu, S.H. Ong, Y. Sun and D.W.K. Wong *et al.*, 2011. Model-based optic nerve head segmentation on retinal fundus images. Proceedings of the 2011 Annual International Conference on IEEE Engineering in Medicine and Biology Society (EMBS'11), August 30-September 3, 2011, IEEE, Boston, Massachusetts, USA., ISBN:978-1-4244-4121-1, pp: 2626-2629.
- Youssif, A.A.H.A.R., A.Z. Ghalwash and A.A.S.A.R. Ghoneim, 2007. Optic disc detection from normalized digital fundus images by means of a vessels direction matched filter. *IEEE. Trans. Med. Imaging*, 27: 11-18.
- Zhang, D., Y. Yi, X. Shang and Y. Peng, 2012. Optic disc localization by projection with vessel distribution and appearance characteristics. Proceedings of the 21st International Conference on Pattern Recognition (ICPR2012), November 11-15, 2012, IEEE, Tsukuba, Japan, pp: 3176-3179.